Journal of
Plankton Research

academic.oup.com/plankt

J. Plankton Res. (2021) 43(4): 527–545. First published online May 31, 2021 https://doi.org/10.1093/plankt/fbab039

ORIGINAL ARTICLE

Zooplankton size spectra and production assessed by two different nets in the subarctic Northeast Pacific

LIAN E. KWONG[1] AND EVGENY A. PAKHOMOV[1,2,3]

[1]DEPARTMENT OF EARTH, OCEAN AND ATMOSPHERIC SCIENCES, UNIVERSITY OF BRITISH COLUMBIA, VANCOUVER, BRITISH COLUMBIA V6T 1Z4, CANADA, [2]INSTITUTE FOR THE OCEANS AND FISHERIES, UNIVERSITY OF BRITISH COLUMBIA, VANCOUVER, BRITISH COLUMBIA V6T 1Z4, CANADA AND [3]HAKAI INSTITUTE, HERIOT BAY, BRITISH COLUMBIA V0P 1H0, CANADA

*CORRESPONDING AUTHOR: kwong@eoas.ubc.ca

Received October 29, 2020; editorial decision May 3, 2021; accepted May 3, 2021

Corresponding editor: Marja Koski

Normalized biomass size spectra (NBSS) are frequently used to describe pelagic communities. However, the underlying structure of NBSS may lead to varying intercepts and slopes when only a portion of the biomass range is sampled. This may be further perpetuated by the sampling efficiency of different gears/mesh sizes. Spatial and seasonal effects of mesh size on zooplankton NBSS and production were evaluated. Zooplankton were collected during winter, spring and summer (2017–2019) between Vancouver Island and Station Papa (50°N, 145°W) using a 64-μm Working Party 2 (WP-2) net and a 236-μm bongo net and analyzed using a bench-top laser optic particle counter. WP-2 and bongo NBSS overlapped in 11 size classes, for which the WP-2 more effectively sampled smaller size classes and converged with the bongo in larger size classes. Differences in NBSS slopes from the two nets were detected, yet no differences in total production. However, the contribution of individual size classes to total production varied spatially and seasonally. Total production in the coastal region exhibited strong seasonal variability. Notably, summer estimates of production in the coastal region were at least 2-fold higher than transitional and open ocean regions. This study suggests that using one mesh size may underestimate zooplankton NBSS and thus production.

KEYWORDS: normalized biomass size spectra; NBSS; size spectra; zooplankton; zooplankton production

available online at academic.oup.com/plankt

INTRODUCTION

Pelagic communities exhibit remarkable predictability when it comes to the distribution of biomass by body size. This feature was first observed with phytoplankton in the marine environment by Sheldon *et al*. (1972). The authors found that the distribution of biomass by body size could be described by a straight line of low negative slope, hypothesizing that this would hold true across all organism sizes within a marine ecosystem. The theory was later formalized as the Biomass Spectra Theory (BST; Kerr and Dickie 2001), and while it is largely accepted to date there are few studies that calculate whole ecosystem size spectra (Blanchard *et al*., 2017). Nevertheless, the BST provides a simple ataxonomic approach by which complex systems can be described and has been applied to assess biomass/energy transfer, productive capacity, environmental change and ecosystem health (Sprules and Goyke, 1994; Trudnowska *et al*., 2020; Heneghan *et al*., 2019; Basedow *et al*., 2014; Blanchard *et al*., 2009).

BST is often expressed as normalized biomass size spectra (NBSS), whereby the biomass in each logarithmically equal size bin is divided by the width of the size bin (Kerr & Dickie 2001). The NBSS is then expressed as the least-squares linear regression between log-transformed normalized biomass and body size, with the coefficients (i.e. slope and intercept) providing insight into ecosystem condition. NBSS slope has long been used as an indicator of trophic transfer efficiency (TTE), though the key factors dictating NBSS slope have long been debated in the literature (Zhou, 2006; Atkinson *et al*., 2020). Detailed knowledge of predator:prey mass ratios (PPMR), trophic level at body size and TTE are required to determine what is dictating NBSS slope (Jennings *et al*., 2002; Atkinson *et al*., 2020). For example, a system with a shallow NBSS slope may indicate high transfer efficiency or large PPMR, which may arise due to the physical accumulation of larger zooplankton (Mehner *et al*., 2018). In contrast, a steep NBSS slope may indicate low transfer efficiency and fewer trophic levels (Zhou, 2006; Wu *et al*., 2014). The NBSS intercept indicates the availability of energy at the base of the food chain (Zhou, 2006; Platt and Denman, 1978; Gaedke, 1993; Blanchard *et al*., 2009). Both NBSS slope and intercept rely heavily on the size range of organisms included (Sprules *et al*., 2016) due to the underlying "lumpy" NBSS structure (i.e. biomass domes and troughs; Fig. 1). Biomass domes are well documented in the literature where they have been shown to represent different trophic or taxonomic groups (e.g. phytoplankton, zooplankton, nekton; Boudreau *et al*., 1991; Rossberg *et al*., 2019; Quiroga *et al*., 2014) and are thought to vary based on predator–prey interactions, leading to oscillations and variable horizontal spacing (Thiebaux and Dickie, 1992; Rossberg *et al*., 2019). Small perturbations in size spectra may also arise due to changes in seasonal production and/or fisheries, leading to oscillations/changes through time or space (Benoît and Rochet, 2004), or due to differences in sampling (Mack *et al*., 2012; Nichols and Thompson, 1991; Trudnowska *et al*., 2020). Further, when the assumptions of fixed prey–predator ratios are relaxed, the biomass domes are manifestations of top-down trophic cascades (Rossberg *et al*., 2019).

Although NBSS for an entire community usually exhibits a slope close to −1 (Kerr and Dickie, 2001), this may not hold true for a subset of the population due to sampling efficiency, the presence of biomass domes and oscillations (e.g. Fig. 1; Gaedke, 1992). For example, a study assessing the NBSS of organisms within the "a" size range would produce a vastly different NBSS intercept and slope than a study of the same community assessing the NBSS of organisms within the "b" or "c" size ranges (Fig. 1). Therefore, it is crucial that studies cover a wide enough size range, particularly when the study objective is to interpolate into smaller and/or larger size classes, as the variability in NBSS slope and intercept may be reduced as the number of size classes increases (Atkinson *et al*., 2020).

Globally, various mesh sizes are used depending on the study objective, with comparison studies recommending a mesh size of 150–156 μm for optimal filtration and capture efficiency of zooplankton (Skjoldal *et al*., 2013; Evans and Sell, 1985; Mack *et al*., 2012). However, a 64-μm mesh net should be used for studies interested in capturing small-bodied zooplankton (i.e. cladocerans, copepod nauplii/larvae and rotifers; Mack *et al*., 2012), which make seasonally important contributions to the pelagic community and thus total zooplankton production (Hopcroft *et al*., 2005).

To date, few estimates of zooplankton production exist in the northeast (NE) subarctic Pacific. Those that do, have been generated using the chitobiase (Sastri and Dower, 2006, 2009; Suchy *et al*., 2016) or the artificial cohort method (Liu and Hopcroft, 2006, 2007) and therefore focus on individual groups and/or species of zooplankton. Studies have begun using size spectra models to quantify zooplankton production in various systems (Basedow *et al*., 2014; Trudnowska *et al*., 2014; Kwong *et al*., 2020), thus providing size-based estimates independent of taxonomic composition. In the NE Pacific, a direct comparison of production estimates using chitobiase and optically derived NBSS [i.e. lab-laser optic particle counter (lab-LOPC)] applied to various empirical growth rate models

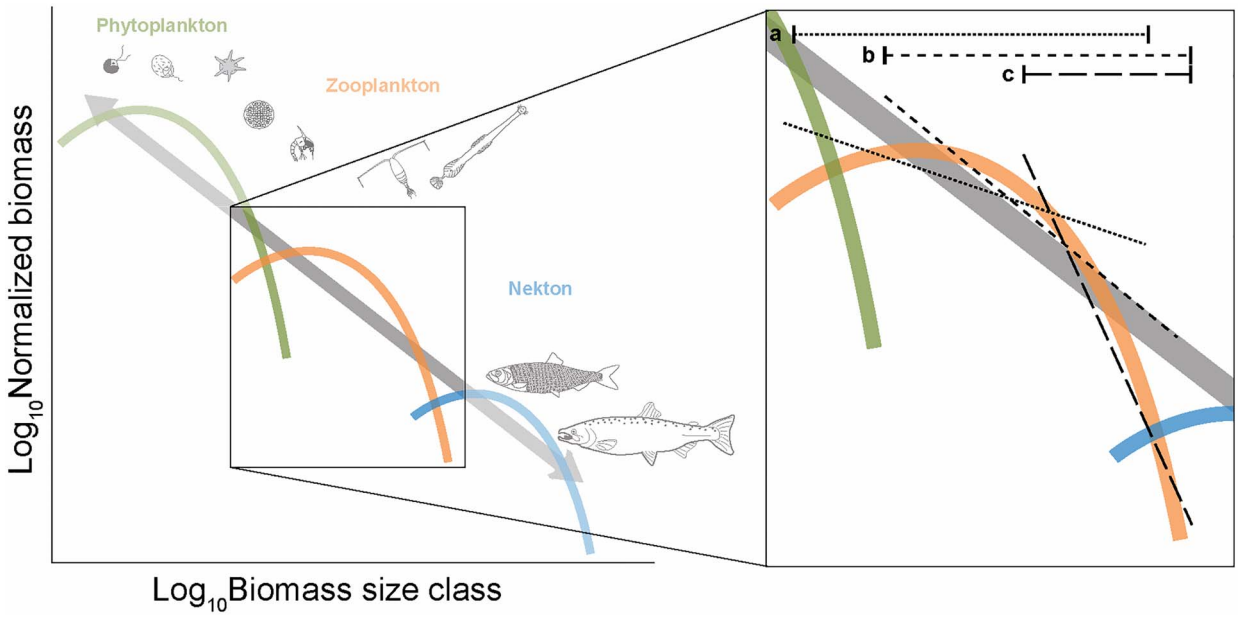

Fig. 1. Conceptual diagram illustrating an ecosystem's NBSS underlying biomass domes. The overview panel displays three NBSS slopes (a, b, c) that may arise when sampling different size ranges of organisms within the zooplankton NBSS. Where the solid gray line represents the systems true NBSS slope.

(Kwong *et al.*, 2020) was recently undertaken. The study reported relatively close agreement between chitobiase and the Hirst–Bunker growth rate model (Hirst and Bunker, 2003) estimates of total production and transfer efficiency. The Hirst–Bunker growth rate model incorporates temperature and chlorophyll-a as an indicator of food quality to quantify marine copepod growth rates. The model assumes that growth is food limited, though the effects of food limitation appear greater on larger copepods. Copepods represent 70–90% of zooplankton abundance globally (Turner, 2004), and the growth rate of pelagic organisms has been shown to scale with body size regardless of taxonomy (Kiørboe and Hirst, 2014). Although, underlying deviations may occur due to species-specific ontogenetic changes. Regardless, the majority of production within the system can likely be captured using this approach as long as system-specific model validation has been performed.

This study quantifies the NBSS of microzooplankton and mesozooplankton spanning a size range of 100–10 000 μm (Table S1) (Calbet, 2008; Makabe *et al.*, 2012) using a bench-top lab-LOPC. We evaluate the differences in zooplankton abundance, biomass, NBSS and production (estimated using the Hirst–Bunker model) from the two nets and produce combined NBSS. We then assess the seasonal variability in NBSS along a coastal-offshore gradient.

METHODS

Study area

This analysis evaluated zooplankton samples ($N = 82$) from the Line P long-term time series in the subarctic NE Pacific Ocean at the seven major stations: P02, P04, P08, P12, P16, P20 and P26 (Fig. 2) between February 2017 and 2019. These stations were selected as they are subject to the most rigorous oceanographic sampling (i.e. physical, chemical and biological sampling).

Line P is a coastal–oceanic transect extending from the southwest coast of Vancouver Island to Station Papa (P26) at 50°N, 145°W. The transect is generally sampled 2–6 times per year and remains one of the oldest deep-ocean time series, providing spatial and temporal (i.e. interannual and seasonal) coverage of chemical, physical and biological properties in the subarctic NE Pacific.

Oceanographic data

At each station, a Seabird SBE911-plus conductivity–temperature–depth (CTD) rosette equipped with 24 Niskin bottles was deployed to measure salinity, temperature, chlorophyll-a and nutrients (i.e. nitrate + nitrite, phosphate, silicate). CTD data were processed by Fisheries and Oceans Canada (DFO) at the Institute of Ocean Sciences (IOS) and aggregated into 1 m depth bins for analysis.

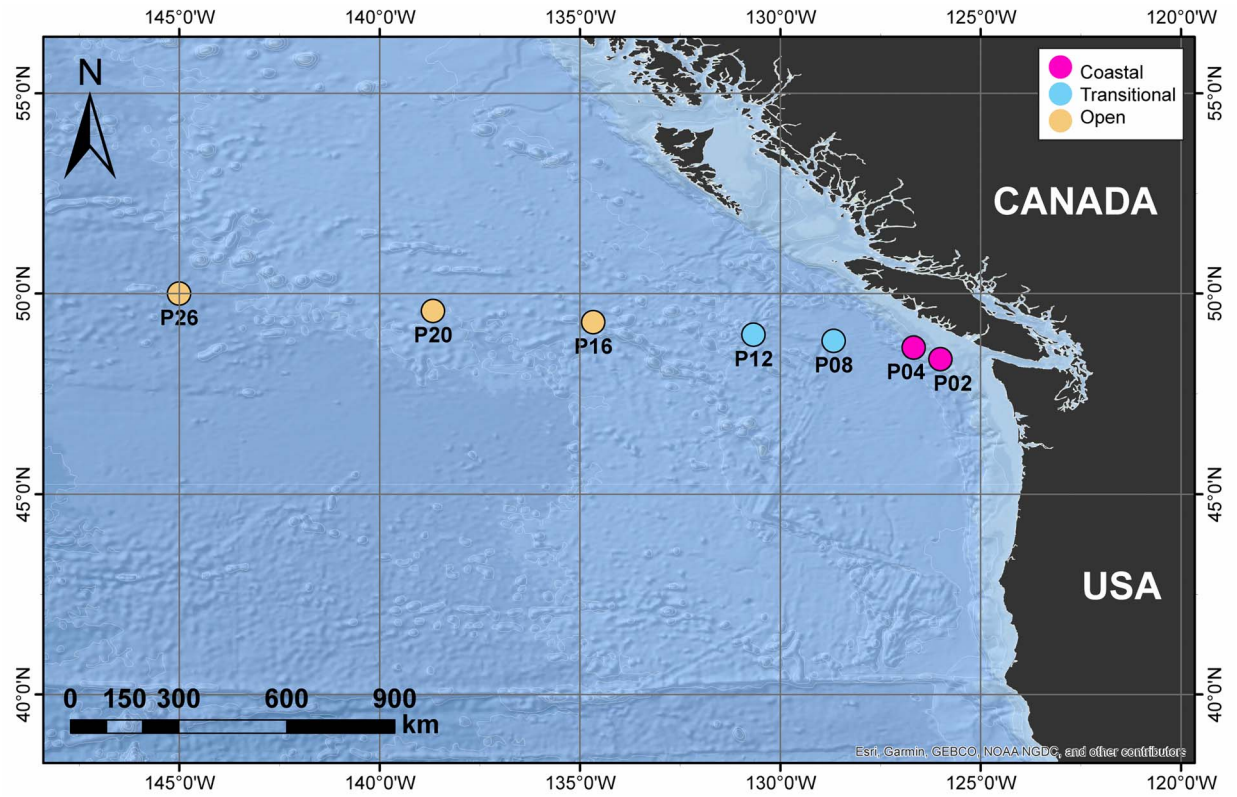

Fig. 2. Map of the major sampling stations (circles) along the Line P transect in the NE Pacific Ocean, separated into region (coastal: P02, P04; transitional: P08, P12; open: P16, P20, P26).

Mixed layer depth (MLD) was estimated by first calculating the potential density for each sampling event using temperature and salinity (Kelley and Richards, 2020). Using the threshold method MLD was calculated according to de Boyer Montégut *et al.* (2004), which identifies the depth at which the potential density deviates from the ocean surface density by ~0.03 kg m^{-3}.

Chlorophyll-a and nutrients (i.e. nitrate + nitrite, phosphate, silicate) were analyzed by the IOS and are publicly available through the DFO Water Properties Portal (www.waterproperties.ca). Chlorophyll-a concentration was determined by filtering a known volume of seawater (500 mL) through a Whatman glass fiber filter and then extracted using 90% acetone for fluorometric determination (Strickland and Parsons, 1972). Depth-integrated concentrations (i.e. chlorophyll-a, nitrate + nitrite, phosphate) within the MLD were calculated using trapezoidal integration (Kelley and Richards, 2020).

Zooplankton

Samples were collected during the winter (February), spring (June) and summer (August/September) from 2017 to 2019 at each station. On some occasions weather constraints made it impossible to deploy one or both nets, leading to some gaps in the data set.

We used bongo (0.56-m mouth and 236-μm mesh) and UNESCO Working Party 2 (WP-2; 0.56-m mouth and 64-μm mesh) nets equipped with TSK flow meters, which were calibrated annually. The WP-2 and bongo nets were vertically towed through the water column from 250 to 0 m depth at speeds of 0.5 and 1 m s^{-1}, respectively. Immediately following collection, samples were fixed in 10% borate-buffered formalin. Bongo net samples were processed by IOS and identified to the lowest taxonomic resolution possible (i.e. species and developmental stage; Mackas, 1992; Mackas *et al.*, 2001). Abundance (ind. m^{-3}) was then calculated using raw counts, proportion of the sample processed and volume filtered.

Fixed WP-2 and bongo net samples were rinsed using 60 and 200-μm mesh sieves to remove formalin, and where necessary, chains of diatoms of nonzooplankton matter (i.e. paint chips, fibers, debris) were removed by hand using a microscope. Samples were then run through a bench-top LOPC (LOPC-660-2 Rolls-Royce Naval Marine) in the lab (hereafter referred to as a lab-LOPC) to obtain estimates of abundance, biomass

and NBSS intercept and slope. The instrument is capable of detecting particles ranging in size from 100 to 35 000 μm (Herman *et al.*, 2004). The lab-LOPC groups particle counts into equal logarithmic size bins based on equivalent spherical diameter (ESD) (Table S1). The instrument was regularly calibrated using three sizes of beads provided by the manufacturer to ensure proper accuracy and precision. The geometric mean ESD for each size bin was calculated and converted to wet weight (mg WW) by assuming ellipsoidal shape (Suthers *et al.*, 2004; Moore and Suthers, 2006). The biomass (mg WW m^{-3}) in each size bin was then converted to normalized biomass (m^{-3}) by dividing the total biomass in each size bin by the width of the bin (Kerr and Dickie, 2001). The first four size classes were excluded from each nets NBSS, as this has been shown to improve the agreement between zooplankton NBSS and taxonomic composition when using nets with varying mesh sizes (Trudnowska *et al.*, 2020). Wet weight/biovolume NBSS were obtained by fitting the data using the least squares regression method expressed as normalized biomass (m^{-3}) against zooplankton size class (mg WW). All references to total biomass are expressed in "wet weight" unless otherwise stated.

The raw NBSS from the WP-2 and bongo nets were combined into single NBSS for each region and season by taking the average of the two nets for each of the 11 overlapping size bins (Table S1).

Production

To estimate production, zooplankton wet weight NBSS were converted to carbon weight NBSS using a ratio of 0.0961 (Kiørboe, 2013). Following Kwong *et al.* (2020) geometric mean carbon weights (Table S1) were used to calculate individual zooplankton growth rate (g_i, d^{-1}) for each size bin (i) according to Hirst and Bunker (2003):

$$\log_{10} g_i = 0.0186\left[\log_{10} T\right] - 0.288\left[\log_{10} BW\right] + 0.417\left[\log_{10} C_a\right] - 1.209$$

Where T is temperature (°C) and C_a is chlorophyll-a concentration (μg L^{-1}). Total zooplankton production per size bin (P_i; mg C m^{-3} d^{-1}) was then calculated by multiplying the biomass in each size bin (B_i; mg C m^{-3}) by the individual growth rate for the given size bin (g_i):

$$P_i = B_i x\, g_i$$

Total zooplankton production (mg C m^{-3} d^{-1}) was then estimated as the sum of production across all size bins. This approach is applied individually to NBSS data from the WP-2, bongo and combined net data to evaluate how different size ranges included in NBSS may influence model estimates.

Statistical analysis

All numerical analyses were conducted in R (R Core Team, 2017). Data were first grouped according to region (coastal, transitional, open ocean; Fig. 2) by evaluating the oceanographic and biological data. Multivariate analyses were conducted on the bongo net taxonomy data using the R packages vegan and clustsig (Whitaker and Christman, 2014; Oksanen *et al.*, 2019). Zooplankton abundances were $\log_{10}$-transformed, and those contributing <5% to the total abundance were excluded. A q-type cluster analysis was performed using a Bray–Curtis similarity matrix and average-linkage clustering (Field *et al.*, 1982). This approach grouped samples exhibiting similar taxonomic composition by station and season.

Analysis of variance (ANOVA) was used to evaluate the differences between $\log_{10}$-transformed abundance, biomass and zooplankton production after testing the assumptions using the Shapiro–Wilks test for normality and Bartlett's test for homogeneity of variance. Tukey honest significant difference (HSD) post hoc tests were performed to evaluate seasonal and regional differences between net types.

To test the differences in NBSS statistically, the NBSS data were rescaled to achieve a y-intercept at the midpoint of the size classes included in each NBSS ($X_{WP\text{-}2} = 0.019$ mg WW; $X_{Bongo} = 1.9$ mg WW; $X_{Combined} = 0.6$ mg WW). This reduces the correlation between NBSS slope and intercept once the least squares regression is fit to the data, allowing for statistical detection of differences in size spectra (Daan *et al.*, 2005). To confirm that the correlation between slope and intercept were sufficiently reduced, and further statistical analyses could be performed, Pearson's correlation was conducted, and the differences in NBSS were evaluated using analysis of covariance (ANCOVA). Pearson's correlation was used to evaluate the relationship between NBSS intercept and slope against $\log_{10}$-transformed oceanographic parameters [i.e. chlorophyll-a, sea surface temperature (SST), MLD salinity, nitrate + nitrite, phosphate, silicate].

RESULTS

Oceanographic environment

The Line P transect exhibited both spatial and temporal variability in measured oceanographic parameters. At all stations, MLD was the deepest during the winter and became shallower during the spring and summer. The seasonal differences in MLD were the greatest at

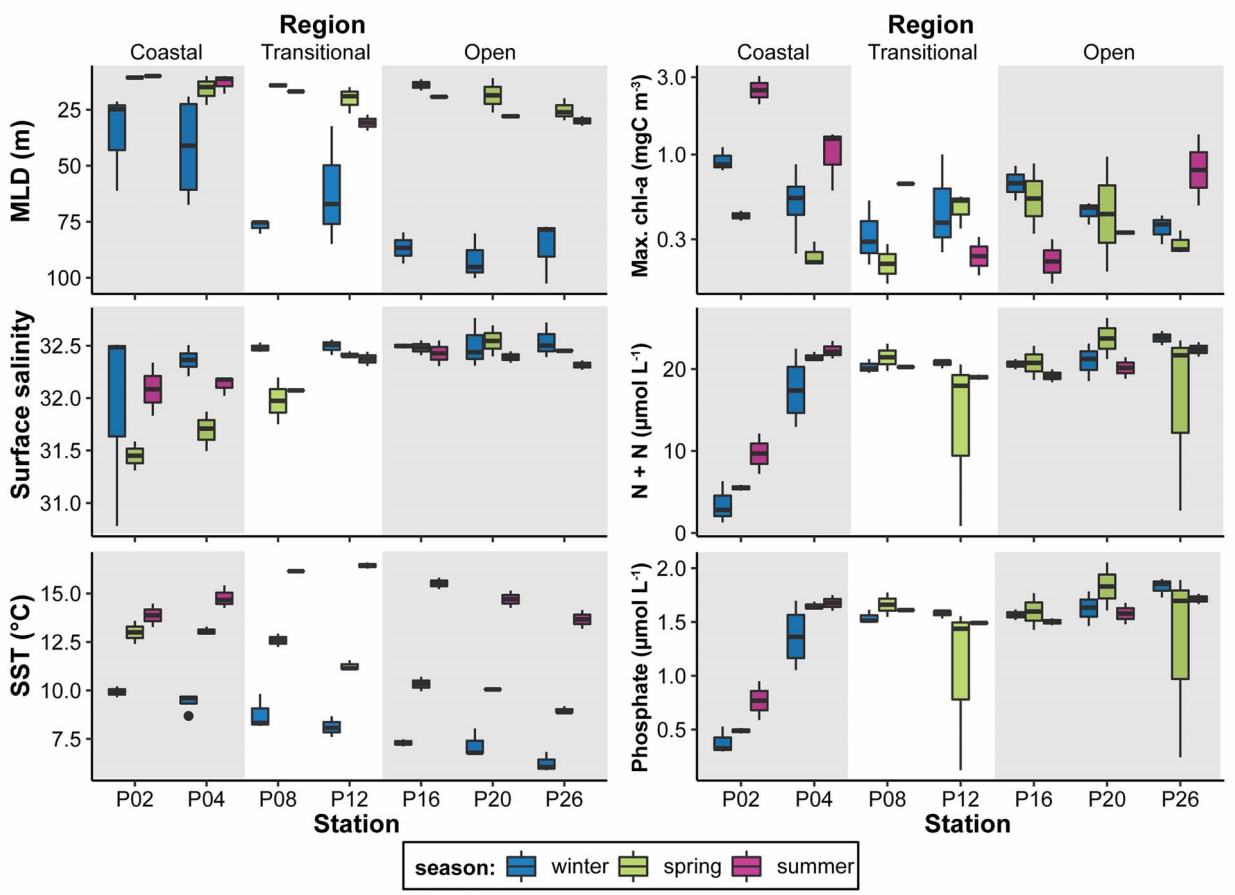

Fig. 3. Boxplot showing the oceanographic parameters: MLD, surface salinity, SST, maximum chlorophyll-a (Max. chlr-a) and depth-integrated (within the MLD) nitrate + nitrite (N + N) and phosphate along the Line P transect by station and season. The shaded areas distinguish between the different oceanographic regions (coastal: P02, P04; transitional: P08, P12; open: P16, P20, P26).

transitional and open ocean stations (Fig. 3). Coastal stations (P02, P04) exhibited less seasonal variability in MLD and SST than transitional (P08, P12) and open ocean (P16–P26) stations (Fig. 3). At coastal stations, we noted less seasonal variability in SST, whereas large differences in SST were observed at the transitional and open ocean stations. In contrast, large seasonal variability in surface salinity at coastal stations was documented, likely corresponding to the spring freshet, with decreasing seasonal variability moving offshore toward P26 (Fig. 3).

Maximum chlorophyll-a exhibited strong seasonality along the entire transect, with the greatest values being observed during the summer along the coast (i.e. P02) and the lowest values occurring in the transitional and open ocean regions (Fig. 3). Seasonal variability in nutrient concentration (i.e. depth integrated within the MLD: nitrate + nitrite, phosphate) was observed at coastal stations, with the lowest concentrations occurring at P02. With the exception of P12 and P26 during the spring, limited seasonal variability in nutrients was observed at the transitional and open ocean stations (Fig. 3). The broad range in nutrient concentrations at P12 and P26 corresponded to strong nutrient depletion in the spring of 2017. Thus, the coastal stations exhibited strong seasonality, the transitional stations moderate seasonality and the open ocean stations low seasonality.

Biological measurements

During the sampling period, the WP-2 net total abundance and biomass of zooplankton ranged from 618 to 24 130 ind. m^{-3} and 20 to 618 mg WW m^{-3}, whereas the bongo estimates ranged from 79 to 1863 ind. m^{-3} and 28 to 655 mg WW m^{-3}. The cluster analysis demonstrated that season and station played a key role in determining zooplankton community similarities in the area, with the stations generally clustering together as coastal (P02, P04), transitional (P08, P12) and oceanic (P16, P20, P26) (Fig. S2).

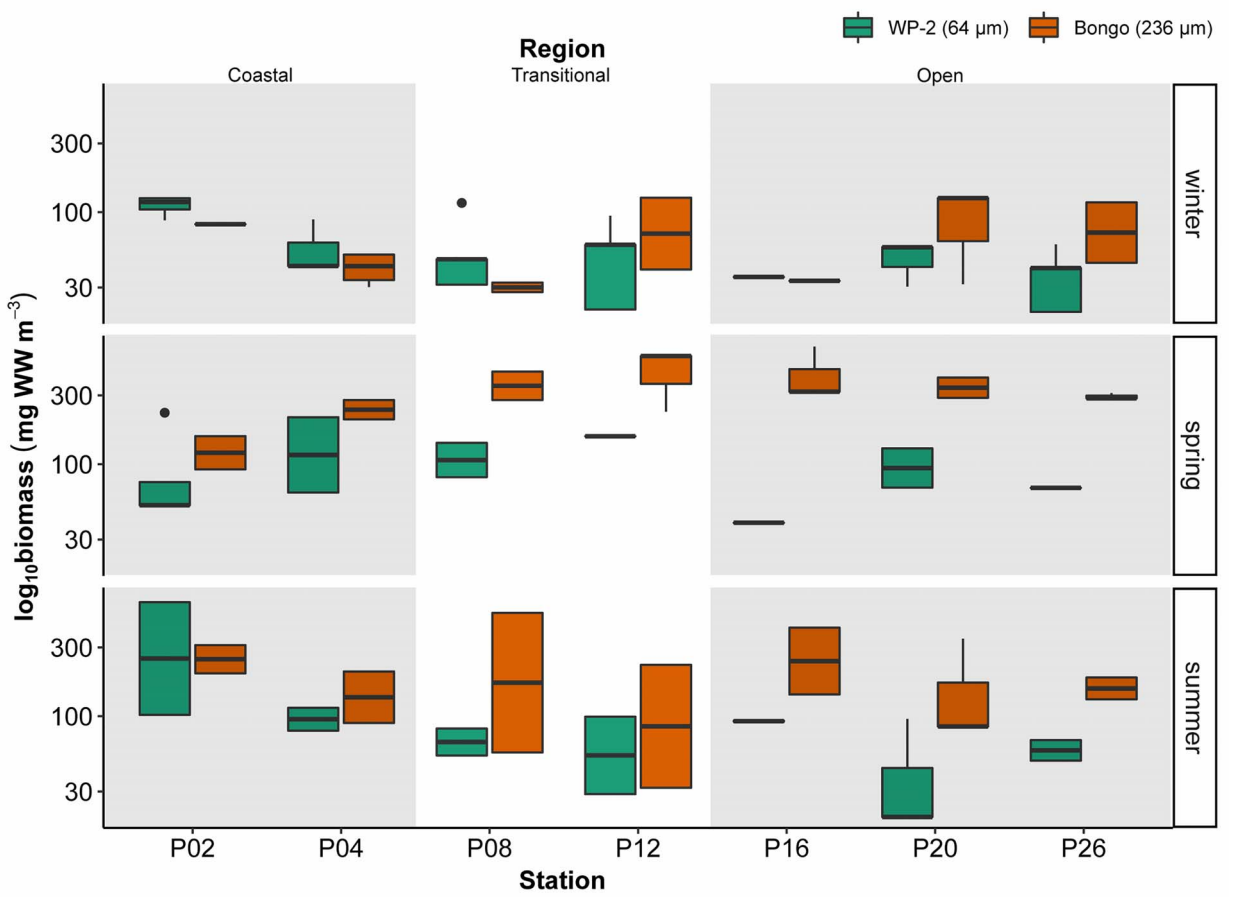

Fig. 4. Boxplot of total zooplankton biomass using the WP-2 (green) and bongo (orange) nets by station, oceanographic region (coastal: P02, P04; transitional: P08, P12; open: P16, P20, P26) and season (winter, spring, and summer) between 2017 and 2019 along the Line P transect.

The abundance (Shapiro–Wilks: $W = 0.98$, $P = 0.08$; Bartlett's test: K-squared = 1.65, $P = 0.20$) and biomass (Shapiro–Wilks: $W = 0.98$, $P = 0.07$; Bartlett's test: K-squared = 4.41, $P = 0.11$) data met the assumptions of ANOVA and Bayesian Information Criterion (BIC) selected for an interaction between region and net. We found significant differences in both total abundance and biomass when comparing the WP-2 and bongo nets (abundance: $P < 0.001$, $F_{1,145} = 493$; biomass: $P < 0.001$; $F_{1,145} = 29$; Table S2), with the WP-2 net consistently capturing higher total abundance (Fig. S1). Regional differences in total abundance were also detected, with the highest zooplankton abundances at coastal stations, followed by transitional and open ocean regions (Tukey HSD; $P < 0.001$). The bongo net captured significantly more total biomass (i.e. wet weight) than the WP-2 net at open ocean stations ($P < 0.001$; Table S3; Fig. 4). No significant differences in biomass estimates between nets at coastal ($P = 0.98$) or transitional ($P = 0.06$) stations were detected (Table S3; Fig. 4).

Normalized biomass size spectra

The NBSS produced by the WP-2 net and bongo nets overlapped for 11 size classes ranging from 0.02 to 2.4 mg WW (Table S1), in which the WP-2 net generally had higher normalized biomass (Fig. 5) and total biomass (Fig. 6). At transitional and open ocean stations during the spring and summer, the WP-2 net captured higher normalized and total biomass for the smaller overlapping size classes and converged with the bongo net in the larger overlapping size classes (Figs 5 and 6). Further, the larger size classes exhibited greater variability (Fig. 5). During the summer at coastal stations, the mean difference between bongo and WP-2 net biomass by size class exhibited large standard error, which was driven by a large bloom at P02 in the summer of 2018. On this occasion, the WP-2 net abundance and biomass was an order of magnitude higher than that of the bongo net (Figs 4 and S1).

When considering only the overlapping size bins (Fig. 6), we detected significant differences in NBSS

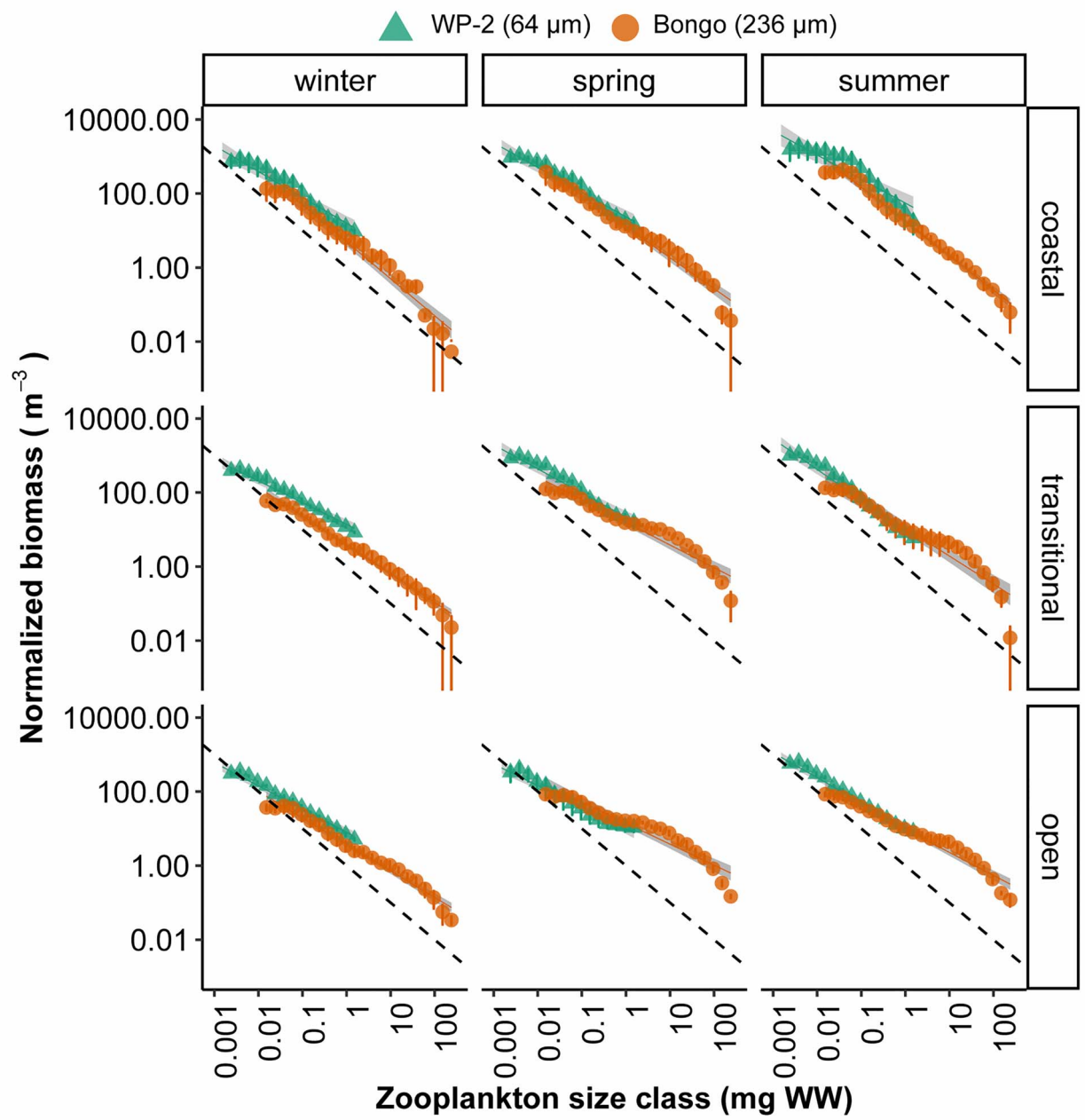

Fig. 5. NBSS expressed as logarithmic size class (wet weight) against log-normalized biomass (m^{-3}) and grouped by net (WP-2 and bongo nets), region (coastal: P02, P04; transitional: P08, P12; open: P16, P20, P26) and season (winter, spring and summer). Samples were collected between 2017 and 2019. Bars indicate ±standard error of the mean, and the dashed line indicates an NBSS slope of −1.

intercept ($P \leq 0.005$), except for the transitional region during the summer ($P = 0.11$; Table S4). NBSS slopes for the overlapping size classes differed significantly during the spring in the transitional ($P = 0.01$) and open ocean ($P = 0.03$) region, and during the summer in the open ocean region ($P < 0.001$), no other significant differences in NBSS slope for the overlapping size classes were detected (ANCOVA; Table S4). The overlapping size classes of the WP-2 and bongo net were averaged and produced a combined NBSS spanning 26 size classes from 0.002 to 240.125 mg WW (Fig. 7).

NBSS slopes (mean: $b_{WP\text{-}2} = -0.5$, $b_{Bongo} = -0.7$; $b_{Combined} = -0.8$; Fig. 8) were generally flatter (closer to 0) than the hypothetical steady state slope of −1 (Fig. 8). The WP-2 NBSS slopes were flatter than those of the bongo net with a few exceptions. Specifically, the bongo

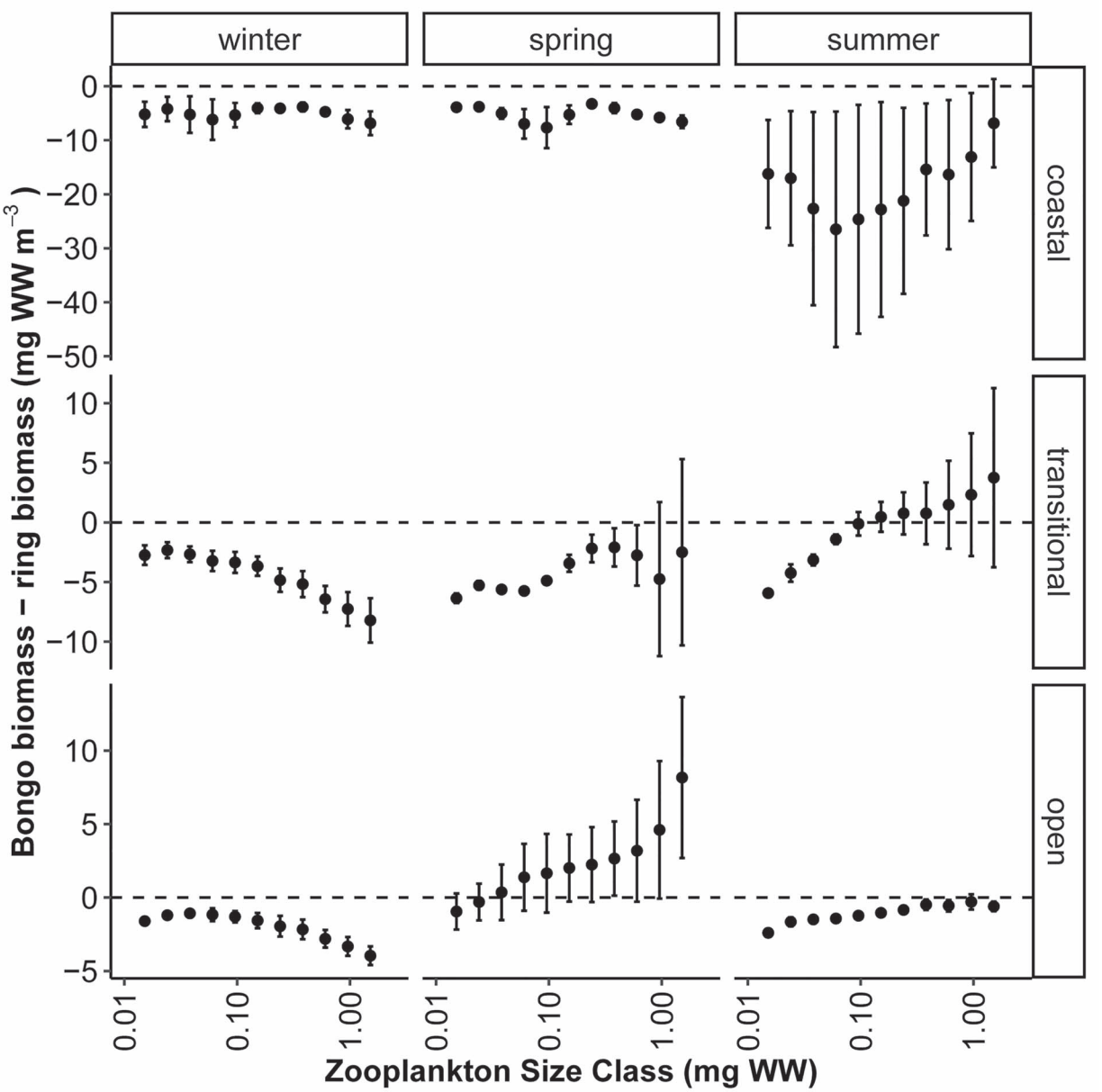

Fig. 6. The difference between bongo and WP-2 total wet weight biomass (mg WW m^{-3}) by log-10 transformed zooplankton size class (mg WW). Samples were collected at major Line P stations between 2017 and 2019 and grouped by region (coastal: P02, P04; transitional: P08, P12; open: P16, P20, P26) and season (winter, spring, summer). Bars indicate ±standard error of the mean. Note: *y*-axis differs across plots due to large differences between net biomass in the coastal region.

slope was flatter than the WP-2 in the transitional region during the spring and summer, and in the open ocean region during the summer, whereas the two nets produced similar slopes in the open ocean region during the spring (Fig. 8).

Rescaled wet weight NBSS met the assumption of normality and homogeneity of variance (Shapiro–Wilks: $W = 0.98$, $P = 0.85$; Bartlett's test: K-squared = 2.18, $P = 0.34$), and Pearson's correlation revealed no significant correlation between intercept and slope for the WP-2 NBSS ($r = -0.10$, $P = 0.98$), bongo NBSS ($r = 0.15$, $P = 0.69$) or combined NBSS ($r = 0.31$, $P = 0.41$; Table 1). BIC selected for a linear model with an interaction between region and net for NBSS slope ($P = 0.02$), and an additive model with region, season and net (i.e. WP-2, bongo, combined) for NBSS intercept ($P < 0.001$;

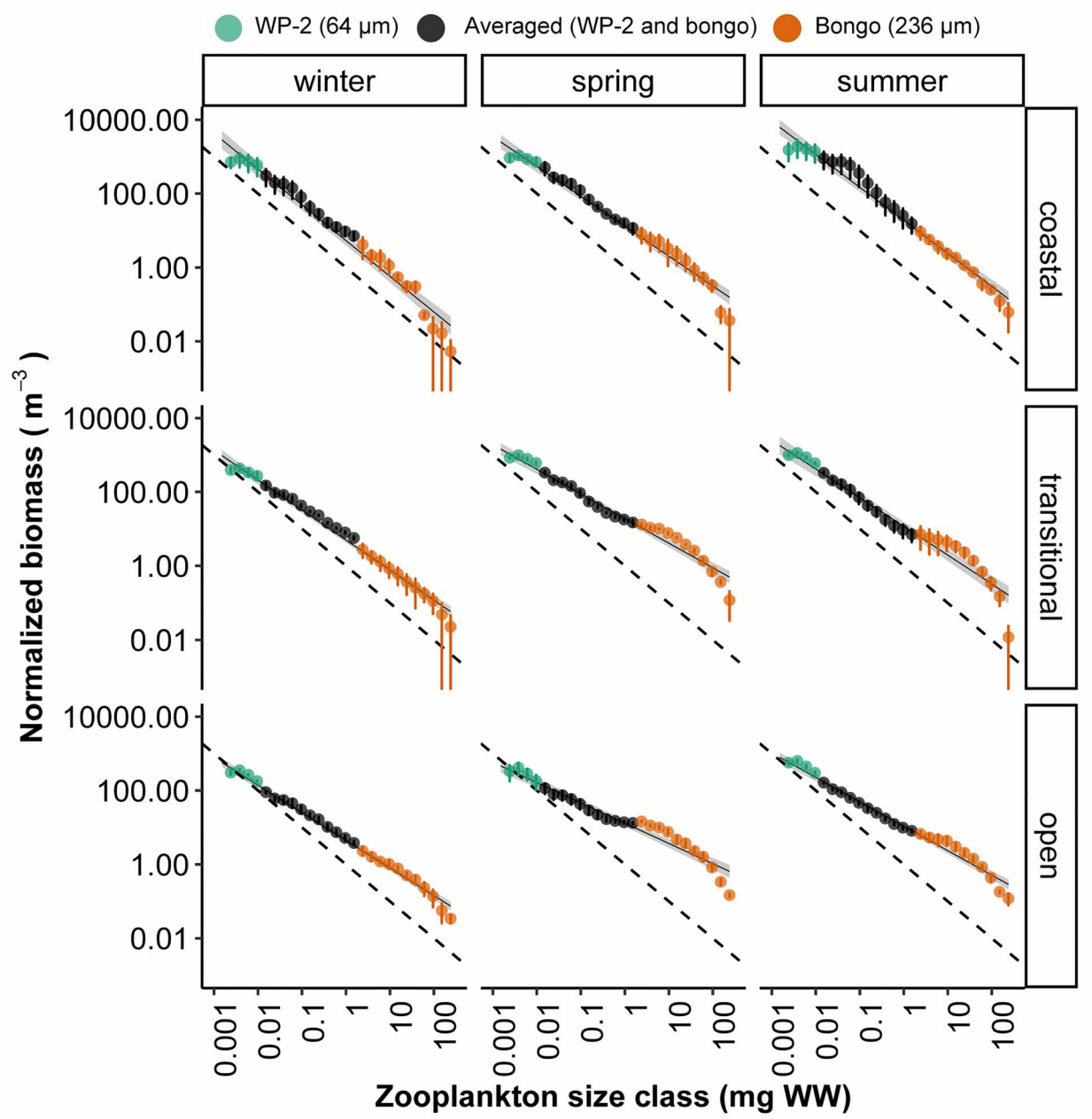

Fig. 7. Combined WP-2 and bongo NBSS expressed as logarithmic size class (wet weight) against log-normalized biomass (m^{-3}) grouped by region (coastal: P02, P04; transitional: P08, P12; open: P16, P20, P26) and season (winter, spring and summer). Samples were collected between 2017 and 2019. Bars indicate ±standard error of the mean.

Table S2). In the coastal region, the NBSS slope of the WP-2 was significantly flatter than the bongo (difference = 0.21; $P < 0.001$) and combined NBSS (difference = 0.19; $P = 0.01$; Table S3). Regional differences were also detected for the bongo and combined NBSS slopes, as coastal NBSS were generally steeper than open NBSS ($P < 0.01$). In addition, bongo NBSS were steeper in coastal regions than in transitional regions ($P \leq 0.01$). We detected significant differences in NBSS intercept by net (i.e. WP-2–bongo, WP-2–combined, bongo–combined; $P = 0.001$), region (open–coastal, open–transitional; $P \leq 0.04$) and season (spring–winter, summer–winter; $P < 0.001$; Tukey HSD; Table S3).

We detected significant correlations between combined NBSS slopes and intercept with physical and chemical parameters (i.e. maximum chlorophyll-a, SST,

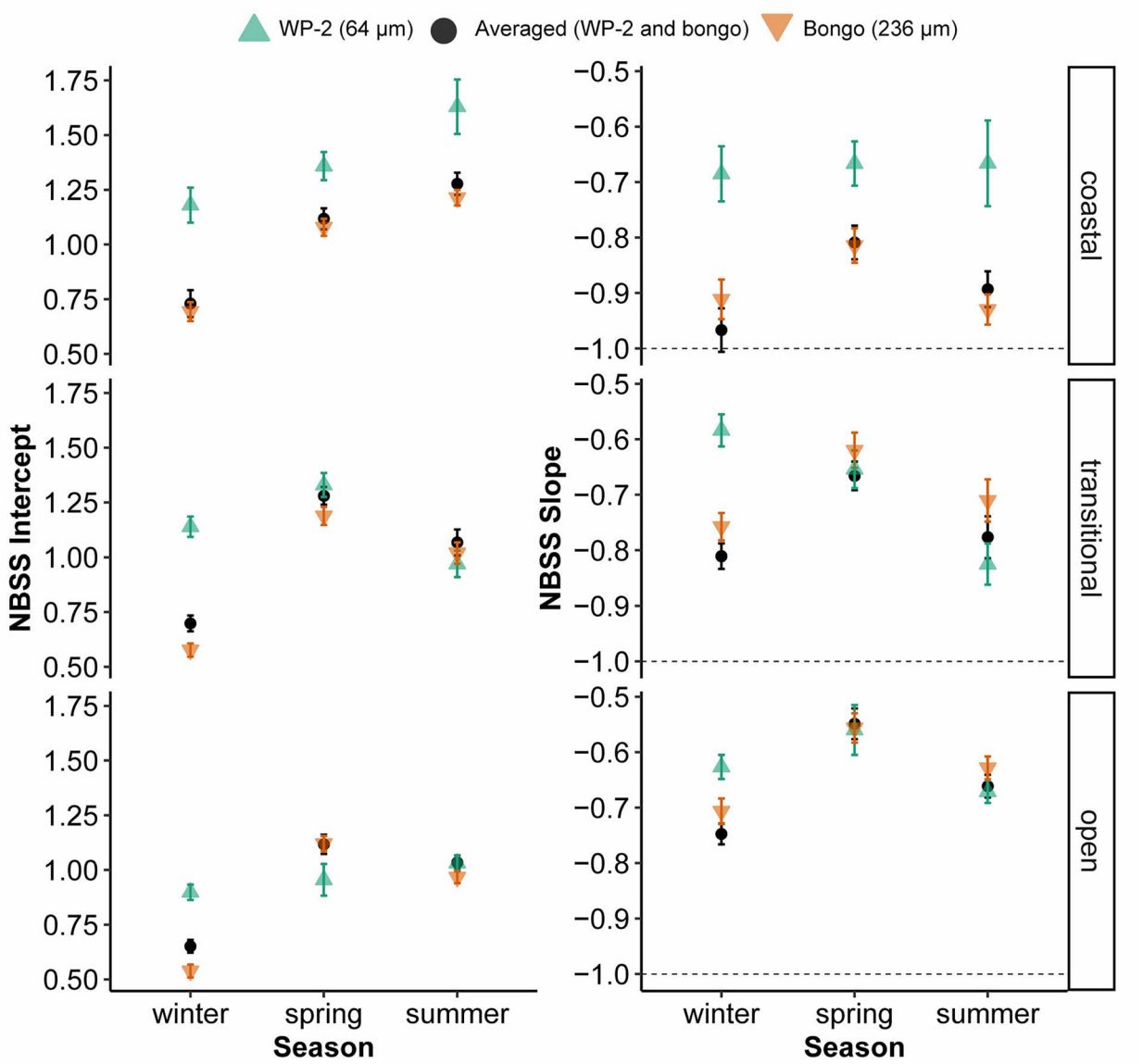

Fig. 8. Wet weight NBSS intercept and slope from the WP-2, bongo and both nets combined by region (coastal: P02, P04; transitional: P08, P12; open: P16, P20, P26) and season (winter, spring and summer). Bars indicate ±standard error of the mean. The dashed line on the right plot indicates NBSS slope of −1.0.

Table 1: Results of Pearson's correlation between rescaled wet weight NBSS intercept and slope for the WP-2, bong, and combined

Data	*t*-value	DF	*P*-value	*R*
WP-2	−0.03	7	0.98	−0.1
Bongo	0.41	7	0.69	0.15
Combined	0.87	7	0.41	0.31

MLD, surface salinity, nutrients; Fig. 9). Specifically, negative relationships were detected between NBSS slope and maximum chlorophyll-a ($r = -0.41$; $P < 0.001$) and SST ($r = -0.46$; $P < 0.001$) and between NBSS intercept and MLD ($r = -0.55$; $P < 0.001$) and surface salinity ($r = -0.43$; $P < 0.001$; Fig. 9). A weak positive relationship was detected between NBSS slope and surface salinity ($r = 0.17$; $P = 0.05$) and all three nutrients

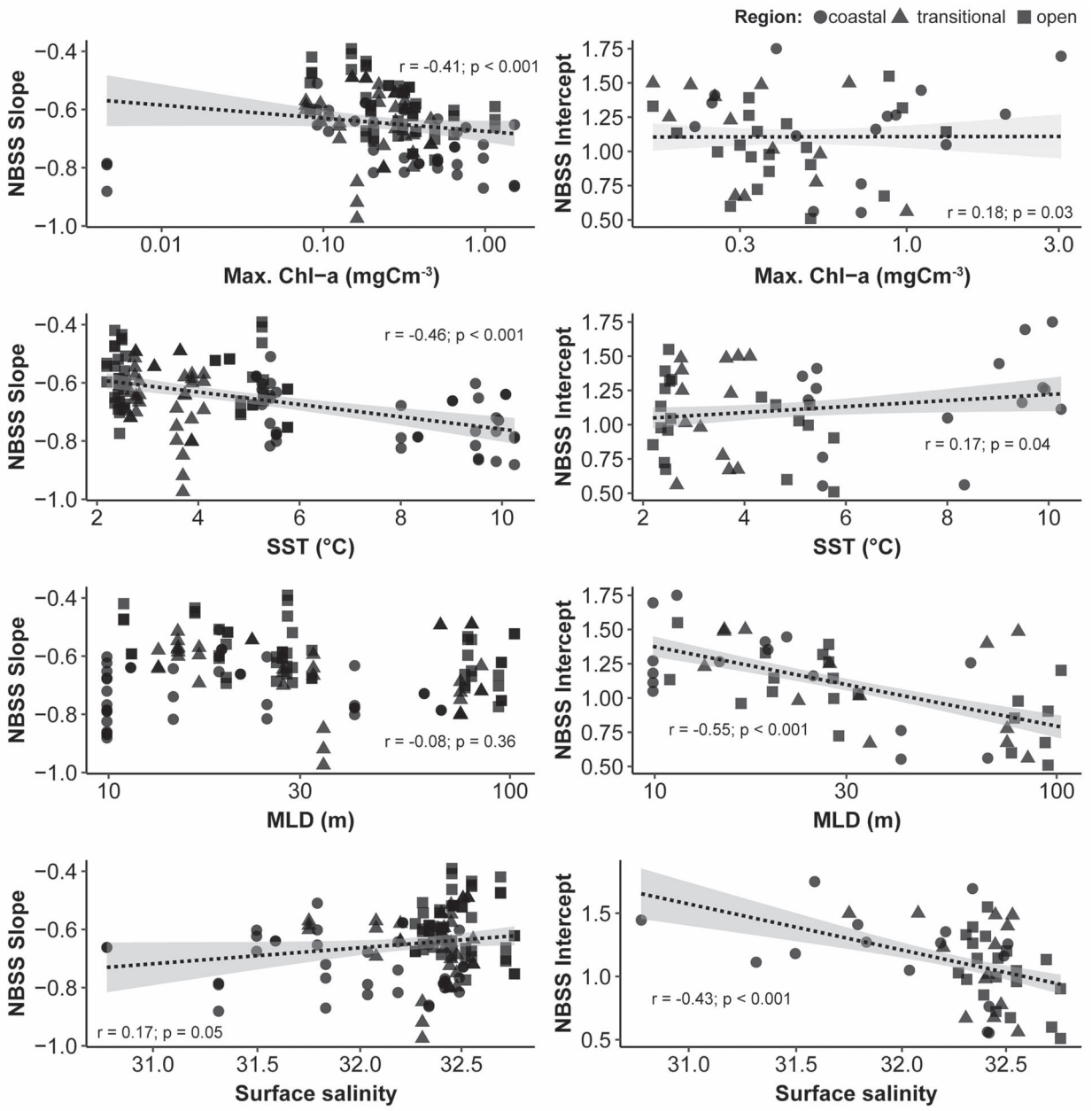

Fig. 9. Pearson's correlations between zooplankton NBSS slope (left) and intercept (right) and maximum chlorophyll-a, SST, MLD and surface salinity between February 2017 and 2019 along Line P. Where the symbol indicates region.

($r \leq 0.24$; $P \leq 0.03$; Fig. S3) and between NBSS intercept and maximum chlorophyll-a ($r = 0.18$; $P = 0.03$) and SST ($r = 0.17$; $P = 0.04$; Fig. 9). NBSS intercept also exhibited a strong positive correlation with all three nutrients ($r \geq 0.43$; $P < 0.001$; Fig. S3).

Zooplankton production

Mean estimates of zooplankton production in the coastal, transitional and open ocean stations were 4.9 mg C m^{-3} d^{-1} (range: 1.9–11.0 mg C m^{-3} d^{-1}), 2.5 mg C m^{-3} d^{-1} (range: 1.1–3.4 mg C m^{-3} d^{-1}) and 2.4 mg C m^{-3} d^{-1} (range: 1.4–3.4 mg C m^{-3} d^{-1}), respectively (Table 2).

Estimates of zooplankton production were consistently higher from the WP-2 net than the bongo net at coastal stations (Table 2). In contrast, transitional and oceanic stations had higher estimates of production from the bongo net during the spring and summer, whereas WP-2

Table 2: Average zooplankton production estimates (±standard error of the mean) using the Hirst and Bunker (2003) growth rate model separated by the WP-2, bongo net and combined estimates

Region	Season	Production (mg C m^{-2} d^{-1})			% of total combined	
		WP-2	Bongo	Combined	WP-2	Bongo
Coastal	Winter	4.91 ± 1.3	2.50 ± 1.0	4.70 ± 1.8	105%	53%
Coastal	Spring	2.98 ± 1.4	1.85 ± 1.0	2.58 ± 1.6	115%	72%
Coastal	Summer	11.02 ± 6.8	4.78 ± 1.4	8.84 ± 4.4	125%	54%
Transitional	Winter	2.46 ± 0.4	1.14 ± 0.3	1.90 ± 0.5	129%	60%
Transitional	Spring	2.09 ± 0.7	3.02 ± 0.6	3.15 ± 1.1	66%	96%
Transitional	Summer	2.32 ± 0.7	2.79 ± 1.5	3.41 ± 1.4	68%	82%
Open	Winter	1.99 ± 0.4	1.38 ± 0.4	2.22 ± 0.6	90%	62%
Open	Spring	2.06 ± 1.0	3.36 ± 0.7	3.44 ± 1.2	60%	98%
Open	Summer	1.95 ± 0.4	2.15 ± 0.4	3.03 ± 0.7	64%	71%
Average		3.53	2.55	3.70	91%	72%
Minimum		1.95	1.14	1.90	60%	53%
Maximum		11.02	4.78	8.84	129%	98%

% of total combined production from the WP-2 and bongo net are also provided (i.e. WP-2 production/Combined production*100).

estimates were higher in the winter (Table 2). Production estimates exhibited a decreasing trend with distance from the coast. The combined NBSS production estimates were generally more similar to the WP-2 in coastal stations, yet more similar to the bongo net in transitional and open ocean areas (Table 2). Notably, average WP-2 estimates of zooplankton production exceeded that of the combined NBSS estimates in the coastal region during all seasons and in the transitional region during the winter (Table 2).

The log-transformed data met the assumption of ANOVA (Shapiro–Wilks: $W = 0.95$, $P = 0.26$; Levene's test: $F_{8,104} = 2.29$, $P > 0.05$). BIC model selection identified that the best-fit model was that including an interaction between region and season ($P = 0.01$; $F_{2,104} = 3.51$; Table S5), as no significant difference in production across nets was observed (i.e. WP-2, bongo, combined; $P = 0.42$; $F_{2,110} = 0.87$). The coastal region exhibited strong seasonality, with a significant increase in production from spring and summer ($P = 0.003$) and a decrease from summer to winter ($P = 0.04$), though no difference in production was observed between winter and spring ($P = 0.99$; Table S6). No significant seasonal changes in production were detected in the transitional ($P \geq 0.99$) or open ocean regions ($P \geq 0.98$; Tukey HSD; Table S6). We detected significant differences in production across regions during the summer. Specifically, production in the coastal region was at least double that of the transitional ($P = 0.009$) and open ocean regions ($P < 0.001$) during the summer (Table S6). All regions exhibited similar seasonal and spatial patterns in total production using all three NBSS (i.e. WP-2, bongo and combined).

Notable differences in the contribution of each NBSS size class were observed across stations and seasons (Figs 10 and S4). For example, during the spring and summer increases in the contribution of larger size classes to zooplankton production were observed at transitional and open ocean stations (Fig. 10). In contrast, during the summer, smaller size classes contributed more to zooplankton production at coastal stations (Fig. 10).

DISCUSSION

This study provides a comparison of zooplankton abundance, biomass, NBSS slope and zooplankton production using two nets along a coastal–open ocean transect over three seasons (i.e. winter, spring, summer). Zooplankton abundance estimates were consistently higher using the WP-2 net (64-μm mesh), whereas biomass estimates varied by region and net type. The WP-2 net generally produced flatter NBSS (i.e. closer to 0) than the bongo net. No significant difference in total zooplankton production estimates using the WP-2, bongo or combined confidence-weighted NBSS were observed. However, spatial (i.e. open ocean estimates were lower than coastal estimates) and seasonal variability in zooplankton production estimates were detected. Below, we discuss the results in the context of the existing literature, separated by the methodological comparison across nets and ecological context. We then discuss how these observations contribute to the existing zooplankton knowledge within the region.

Methodological considerations

The lab-LOPC is unable to distinguish between dead and living organisms. Therefore, estimates of zooplankton production assume that all organisms captured in the nets were continually growing, potentially overestimating zooplankton production. The Hirst and Bunker (2003)

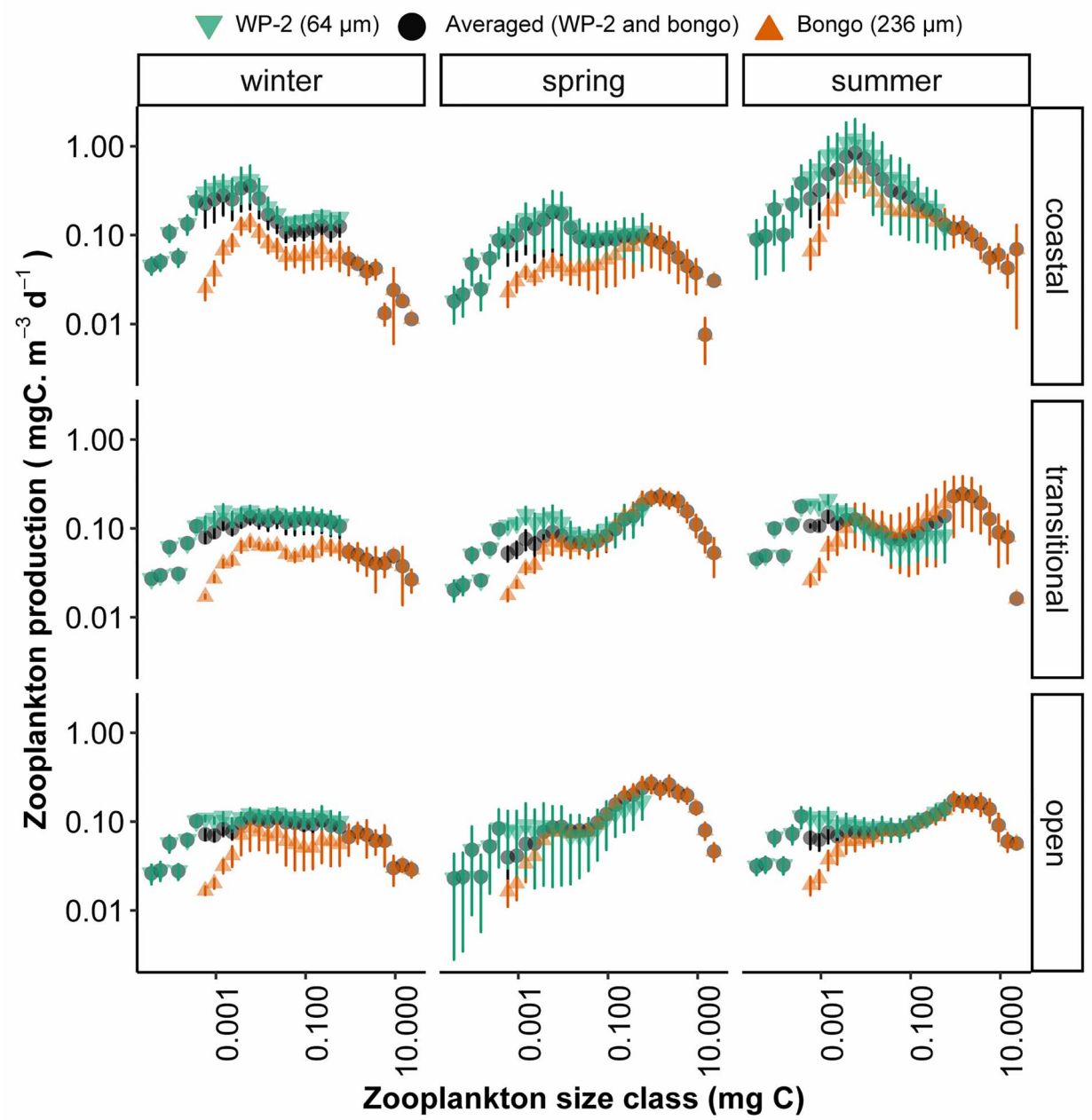

Fig. 10. Average zooplankton production estimates using the Hirst–Bunker growth rate model (Hirst and Bunker, 2003) by carbon weight size class, net (i.e. WP-2, bongo, combined), region (coastal: P02, P04; transitional: P08, P12; open: P16, P20, P26) and season (winter, spring and summer) along the Line P transect from 2017 to 2019. Bars indicate ±standard error of the mean.

growth rate model is based on the growth rates of marine planktonic copepods (sac and broadcaster spawners), which generally make up 70–90% of the zooplankton community numerically (Turner, 2004). This may therefore lead to over−/underestimations in production estimates due to differential growth rates for noncrustacean zooplankton. However, the technique has previously been validated in Saanich Inlet, British Columbia (Kwong *et al.*, 2020), where the authors reported reasonable agreement between chitobiase-based estimates of the crustacean community production and estimates using the lab-LOPC-resolved crustacean NBSS coupled with the Hirst and Bunker growth rate model (Hirst and Bunker, 2003).

Regionalization

The stations were grouped into coastal (P02, P04), transitional (P08, P12) and open ocean (P16, P20, P26), based on hydrographic and taxonomic properties. The coastal region exhibited strong seasonal variability in chlorophyll-a and salinity, relatively high temperature and low macronutrient concentrations. The transitional region experienced coastal and offshore influences, with large seasonal differences in MLD, SST and surface salinity and relatively high macronutrient concentrations. The open ocean region exhibited strong seasonality in MLD and SST driven by strong winter storms (i.e. wind stress and heat flux; Kang *et al.*, 2010). Characteristic of high-nutrient, low-chlorophyll-a regions, the open ocean region experienced limited seasonal variability in chlorophyll-a and high macronutrient concentrations, which extended into the transitional region. These conditions arise due to iron limitation, which has been shown to influence the physiology and size distribution of chlorophyll at the P26 (Crawford *et al.*, 2003; Harrison *et al.*, 2004; Whitney *et al.*, 2005). This corresponds to a gradient in the phytoplankton composition along Line P, as larger cells (i.e. diatoms) have been shown to dominate the coastal portion of the transect, particularly during the spring and summer, and small cells (i.e. flagellates) dominate the offshore areas (Asher *et al.*, 2017; Peña and Varela, 2007). Low concentrations of large diatom cells are maintained throughout the year along the transitional and oceanic portion of the transect where their growth is iron limited (Peña and Varela, 2007). Thus, this regional variability has implications for higher trophic levels (Espinasse *et al.*, 2020).

Net comparison: abundance, biomass, NBSS, production

We validate the findings of several studies that mesh size influences the biomass and abundance of the zooplankton effectively captured (Skjoldal *et al.*, 2013; Evans and Sell, 1985; Nichols and Thompson, 1991; Makabe *et al.*, 2012). Specifically, finer mesh sizes more effectively capture smaller zooplankton at the cost of undersampling larger zooplankton, which are more effectively captured by coarser mesh sizes (Skjoldal *et al.*, 2013; Evans and Sell, 1985; Moriarty and O'Brien, 2013). While the discrepancies in total abundance and biomass of zooplankton captured by plankton nets has been thoroughly documented in the literature, zooplankton size distributions are seldom intercompared (Nichols and Thompson, 1991; Atkinson *et al.*, 2020). Studies have demonstrated differential capture of various life stages and total abundance of small zooplankton depending on mesh size (Nichols and Thompson, 1991; Mack *et al.*, 2012) and convergence of NBSS slopes when the first four size bins are dropped from NBSS (Trudnowska *et al.*, 2020).

In this study, the WP-2 and bongo nets overlapped in 11 NBSS size classes ranging from 0.02 to 2.4 mg WW, demonstrating differential size capture by the two mesh sizes reflected in NBSS. Within the overlapping size classes, the WP-2 captured more biomass in smaller size classes and converged with the bongo net in the larger overlapping size classes. Thus, the bongo net was consistently under sampling biomass in the overlapping size classes. Although we removed the four smallest size bins from each net's NBSS (Trudnowska *et al.*, 2020), the NBSS slopes were flatter (i.e. less negative) and the intercepts higher from the WP-2 net. This suggests that each net was sampling a different portion of the biomass dome within the community NBSS (Fig. 1). Specifically, the WP-2 covered a flatter portion of the dome (e.g. "a" in Fig. 1), and the bongo net covered the steeper portion of the dome (e.g. "b" in Fig. 1).

The discrepancy between NBSS slope and intercept is reduced moving along the coastal–oceanic gradient. Suggesting that under increasing micronutrient limitation (e.g. iron limitation), the troughs between biomass domes become suppressed and on occasion dissipate entirely (Rossberg *et al.*, 2019). More intensive studies are recommended to confirm this hypothesis, with more frequent sampling and replication during the spring and summer months, particularly in the highly dynamic coastal regions when phytoplankton growth is seasonally limited the availability of macronutrients. These discrepancies caution the use of a single-net mesh to derive community-level changes in NBSS on spatial and temporal gradients, particularly in dynamic coastal regions.

Zooplankton production estimates from the WP-2 and bongo net were in close agreement during the spring and summer in transitional and open ocean regions in the overlapping size classes. However, the WP-2 estimates were higher in overlapping size classes during the winter in all regions. Similarly, total zooplankton production estimates from the two nets were in close agreement in transitional and open ocean regions during the spring and summer, whereas the estimates from the two nets differed in the winter (all regions) and during all three seasons in the coastal region. These findings highlight the seasonal and spatial variability in the contribution of different zooplankton size classes to total production. In the subarctic Pacific, studies have demonstrated the spatial and temporal variability in growth rates of various stages of copepods using the artificial cohort method (Liu and Hopcroft, 2006, 2007). These studies reported a decrease in growth rate with increasing size, suggesting that in a system numerically dominated by smaller copepods (i.e. steep NBSS), production may be substantially

higher than in systems dominated by larger copepods (i.e. shallow NBSS). In Kingston Harbor, Jamaica, Hopcroft *et al.* (1998) used two nets (64 and 200 μm) to demonstrate that smaller individuals (i.e. <450 μm in length) made up 67% of the total zooplankton production, thus exceeding their biomass contribution. The net abundance/biomass and NBSS data further support this, as slopes were steeper at coastal stations (i.e. greater dominance of smaller zooplankton) and flatter in open ocean stations (i.e. greater dominance of rare larger zooplankton, increased biomass recycling). Therefore, although the differences in production estimates across nets were not significant, overlooking smaller size class may lead to substantial underestimates in zooplankton production depending on the region and season.

Ecological implications

Estimates of zooplankton abundance and biomass were consistent, yet slightly lower, than reported in previous studies in the NE subarctic Pacific, 193–5067 ind. m^{-3} and 16–2600 mg WW m^{-3}, respectively (Sastri and Dower, 2009; MacKas and Tsuda, 1999; Saito *et al.*, 2011), with notable seasonal and spatial differences (McAllister, 1961). Zooplankton abundance decreased moving away from the coast, whereas no regional trend in total biomass was detected. This would suggest that smaller zooplankton were relatively more abundant in coastal areas, explaining higher intercepts, whereas rare large zooplankton more prevalent in open ocean areas of the subarctic Pacific (Espinasse *et al.*, 2020). Similarly, positive coastal–offshore trends in NBSS slopes have been documented in the Bay of Biscay (Vandromme *et al.*, 2014) and Abrolhos Bank (Marcolin *et al.*, 2013), although the studies did not extend as far from the coast as in the present study.

The coastal–offshore gradient in NBSS slope suggests that the open ocean region experiences a higher degree of biomass recycling maintained by multiple trophic levels/-long food chains and likely lower PPMRs (Zhou, 2006; Armengol *et al.*, 2019). Along Line P, nitrogen isotopes have been used to demonstrate that food chain length increases moving away from the coast (Wu *et al.*, 1997). Based on macronutrient and chlorophyll-a concentrations (Fig. 3), the iron limitation in the oceanic portion of Line P transect ultimately limits phytoplankton growth (Harrison *et al.*, 2004; Whitney *et al.*, 2005). Therefore, phytoplankton at open ocean stations rely on zooplankton-mediated recycling of iron for growth (Richon *et al.*, 2020). In contrast, the steeper NBSS (albeit flatter than −1) in coastal areas were likely driven by a greater contribution of small zooplankton, fewer trophic levels and larger PPMRs (Barnes *et al.*, 2010). However, the NBSS also exhibit seasonal variability in the region, which were likely driven by changes in macronutrient concentration/food availability (García-Comas *et al.*, 2016; San Martin *et al.*, 2006) associated with bloom or mortality events (Atkinson *et al.*, 2020). For example, following the onset of a phytoplankton bloom, an increase in biomass is expected to propagate through the smaller size classes initially causing the NBSS to steepen. Once the small zooplankton have consumed the majority of the phytoplankton they will experience a decrease in abundance and biomass, whereas the larger size classes seemingly "catch up," resulting in a flatter NBSS slope as larger zooplankton begin to dominate (Nogueira *et al.*, 2004). This would continue until the system eventually returns to a steady state. However, Atkinson *et al.* (2020) observed the opposite trend with shallowing of the NBSS slope prior to the bloom and steepening of the NBSS in the late summer. This would suggest that steepening of the NBSS slope was related to progressive nutrient stress within the system. To detect such fine scale changes in NBSS throughout a bloom event, frequent sampling would be required to detect pre- and postbloom changes in NBSS.

Zooplankton production estimates decreased with increasing distance from the coast and seasonal variability in production was only detected in the coastal region. This coastal–oceanic gradient in zooplankton production has previously been demonstrated in the Mediterranean Sea (Saiz *et al.*, 1999). Estimates of zooplankton production in the present study were of similar magnitude as past estimates from chitobiase within the region (1.8–9.97 mg C m^{-3} d^{-1}; Sastri *et al.*, 2012; Sastri and Dower, 2009). No directly comparable estimates of zooplankton production exist along the Line P transect, though initiatives are currently underway to provide crustacean production estimates using the chitobiase approach. Regardless, the spatial and seasonal patterns were consistent with past phytoplankton studies and net community production (NCP) studies in the region (Izett *et al.*, 2018; Hamme *et al.*, 2010; Giesbrecht *et al.*, 2012). Izett *et al.* (2018) observed strong correlations between NCP, chlorophyll-a, SST and MLD. However, the relationship did not hold under periods of macro- and micronutrient limitation, as is the case in the oceanic portion of the Line P transect (i.e. iron limitation) and on a seasonal basis in the coastal region. The magnitude of change in zooplankton production on a seasonal basis was most pronounced at coastal stations, with seasonal variability in production in the transitional and open ocean regions. This finding indicates that while primary and secondary producers are closely linked, using primary production to infer higher trophic level productivity and distribution may lead to overestimations. Primary producers (i.e. phytoplankton) have been

extensively represented in ecosystem modeling (e.g. Cheung *et al.*, 2010; Lotze *et al.*, 2019). In the last decade the implications of excluding and/or misrepresenting zooplankton in ecosystem models have received more attention (Heneghan *et al.*, 2016; Everett *et al.*, 2017). More recent ecosystem models excluding zooplankton, cite them as a source of error and/or model limitation (Lotze *et al.*, 2019), suggesting that their inclusion in future models will sharpen projections (Cheung *et al.*, 2016).

CONCLUSIONS

Given the underlying structure of NBSS, this study supports the findings of Atkinson *et al.* (2020) demonstrating that a single mesh size should not be used to infer whole zooplankton community size spectra, rather multiple sampling gears with various mesh sizes should be employed. While the single mesh size approach still provides a valuable "snap-shot" or an index of the pelagic system's secondary production, it has strong limitations in inferring biomass and/or production of size classes beyond the catchability of the used mesh (e.g. micronekton or fish). Furthermore, the seasonal and regional variability in the contribution of different size classes to total production suggests that studies focusing exclusively on production rates of larger zooplankton may substantially underestimate secondary production. Spatial variability in NBSS slope and zooplankton production estimates warrants further investigation of micronutrient limitation influence on extended phytoplankton–zooplankton NBSS with more frequent sampling capturing ecosystem seasonality.

SUPPLEMENTARY DATA

Supplementary data can be found at *Journal of Plankton Research* online.

ACKNOWLEDGEMENTS

We would like to thank the Institute of Ocean Sciences (IOS) for their dedication to sampling, analysis and data archiving of the Line P program. Thank you to Fisheries and Oceans Canada (DFO) and the CGS John P. Tully and CGS Sir Wilfrid Laurier crews for funding and supporting this ongoing research initiative. Special thanks to Marie Robert, Moira Galbraith and Theresa Venello; without them this project would not have been possible. Thank you to Dr Tetjana Ross, Dr Murdoch McAllister, Dr Brian Hunt, Dr Juliano Palacios-Abrantes, Katie R.N. Florko and our three anonymous reviewers for providing comments.

FUNDING

Strategic NSERC (STPGP 478978); NSERC CGS-D to L.E.K.; University of British Columbia Four Year Fellowship to L.E.K.

REFERENCES

Armengol, L., Calbet, A., Franchy, G., Rodríguez-Santos, A., and Hernández-León, S. (2019) Planktonic food web structure and trophic transfer efficiency along a productivity gradient in the tropical and subtropical Atlantic Ocean. *Sci. Rep.*, **9**, 1–19.

Asher, E., Dacey, J. W., Ianson, D., Pena, A., and Tortell, P. D. (2017) Concentrations and cycling of DMS, DMSP, and DMSO in coastal and offshore waters of the Subarctic Pacific during summer, 2010-2011. *J. Geophys. Res. Ocean.*, **122**, 1–22.

Atkinson, A., Lilley, M. K. S. S., Hirst, A. G., McEvoy, A. J., Tarran, G. A., Widdicombe, C., Fileman, E. S., Woodward, E. M. S. *et al.* (2020) Increasing nutrient stress reduces the efficiency of energy transfer through planktonic size spectra. *Limnol. Oceanogr.*, **6**, 422–437.

Barnes, C., Maxwell, D., Reuman, D. C., and Jennings, S. (2010) Global patterns in predator-prey size relationships reveal size dependency of trophic transfer efficiency. *Ecology*, **91**, 222–232.

Basedow, S. L., Zhou, M., and Tande, K. S. (2014) Secondary production at the Polar Front, Barents Sea, August 2007. *J. Mar. Syst.*, **130**, 147–159.

Benoît, E. and Rochet, M. J. (2004) A continuous model of biomass size spectra governed by predation and the effects of fishing on them. *J. Theor. Biol.*, **226**, 9–21.

Blanchard, J. L., Heneghan, R. F., Everett, J. D., Trebilco, R., and Richardson, A. J. (2017) From bacteria to whales: using functional size spectra to model marine ecosystems. *Trends Ecol. Evol.*, **32**, 174–186.

Blanchard, J. L., Jennings, S., Law, R., Castle, M. D., McCloghrie, P., Rochet, M. J., and Benoît, E. (2009) How does abundance scale with body size in coupled size-structured food webs? *J. Anim. Ecol.*, **78**, 270–280.

Boudreau, P. R., Dickie, L. M., and Kerr, S. R. (1991) Body-size spectra of production and biomass as system-level indicators of ecological dynamics. *J. Theor. Biol.*, **152**, 329–339.

de Boyer Montégut, C., Madec, G., Fischer, A. S., Lazar, A., and Iudicone, D. (2004) Mixed layer depth over the global ocean: an examination of profile data and a profile-based climatology. *J. Geophys. Res. C Ocean.*, **109**, 1–20.

Calbet, A. (2008) The trophic roles of microzooplankton in marine systems. *ICES J. Mar. Sci.*, **65**, 325–331.

Cheung, W. W. L., Lam, V. W. Y., Sarmiento, J. L., Kearney, K., Watson, R., Zeller, D., and Pauly, D. (2010) Large-scale redistribution of maximum fisheries catch potential in the global ocean under climate change. *Glob. Chang. Biol.*, **16**, 24–35.

Cheung, W. W. L., Jones, M. C., Reygondeau, G., Stock, C. A., Lam, V. W. Y., and Frölicher, T. L. (2016) Structural uncertainty in projecting global fisheries catches under climate change. *Ecol. Modell.*, **325**, 57–66.

Crawford, D. W., Lipsen, M. S., Purdie, D. A., Lohan, M. C., Statham, P. J., Whitney, F. A., Putland, J. N., Johnson, W. K., *et al.* (2003) Influence of zinc and iron enrichments on phytoplankton growth in the northeastern subarctic Pacific. *Limnol. Oceanogr.*, **48**, 1583–1600.

Daan, N., Gislason, H., Pope, J. G., and Rice, J. C. (2005) Changes in the North Sea fish community: evidence of indirect effects of fishing? *ICES J. Mar. Sci.*, **62**, 177–188.

Espinasse, B., Hunt, B. P. V., Batten, S. D., and Pakhomov, E. A. (2020) Defining isoscapes in the Northeast Pacific as an index of ocean productivity. *Glob. Ecol. Biogeogr.*, **29**, 246–261.

Evans, M. S. and Sell, D. W. (1985) Mesh size and collection characteristics of 50-cm diameter conical plankton nets. *Hydrobiologia*, **122**, 97–104.

Everett, J. D., Baird, M. E., Buchanan, P., Bulman, C., Davies, C., Downie, R., Griffiths, C., Heneghan, R., *et al.* (2017) Modeling what we sample and sampling what we model: challenges for zooplankton model assessment. *Front. Mar. Sci.*, **4**, 1–19.

Field, J. G., Clarke, K. R., and Warwick, R. M. (1982) A practical strategy for analysing multispecies distribution patterns. *Mar. Ecol. Prog. Ser.*, **8**, 37–52.

Gaedke, U. (1993) Ecosystem analysis based on biomass size distributions: a case study of a plankton community in a large lake. *Limnol. Oceanogr.*, **38**, 112–127.

Gaedke, U. (1992) The size distribution of plankton biomass in a large lake and its seasonal variability. *Limnol. Oceanogr.*, **37**, 1202–1220.

García-Comas, C., Sastri, A. R., Ye, L., Chang, C. Y., Lin, F. S., Su, M. S., Gong, G. C., and Hsieh, C. H. (2016) Prey size diversity hinders biomass trophic transfer and predator size diversity promotes it in planktonic communities. *Proc. R. Soc. B Biol. Sci.*, **283**, 20152129.

Giesbrecht, K. E., Hamme, R. C., and Emerson, S. R. (2012) Biological productivity along line P in the subarctic Northeast Pacific: in situ versus incubation-based methods. *Global Biogeochem. Cycles*, **26**, 1–13.

Hamme, R. C., Webley, P. W., Crawford, W. R., Whitney, F. A., Degrandpre, M. D., Emerson, S. R., Eriksen, C. C., Giesbrecht, K. E., *et al.* (2010) Volcanic ash fuels anomalous plankton bloom in subarctic Northeast Pacific. *Geophys. Res. Lett.*, **37**, 1–5.

Harrison, P. J., Whitney, F. A, Tsuda, A., Saito, H., and Tadokoro, K. (2004) Nutrient and plankton dynamics in the NE and NW gyres of the subarctic Pacific Ocean. *J. Oceanogr.*, **60**, 93–117.

Heneghan, R. F., Hatton, I. A., and Galbraith, E. D. (2019) Climate change impacts on marine ecosystems through the lens of the size spectrum. *Emerg. Top. Life Sci.*, **3**, 233–243.

Heneghan, R. F., Everett, J. D., Blanchard, J. L., and Richardson, A. J. (2016) Zooplankton are not fish: improving zooplankton realism in size-Spectrum models mediates energy transfer in food webs. *Front. Mar. Sci.*, **3**, 1–15.

Herman, A. W., Beanlands, B., and Phillips, E. F. (2004) The next generation of optical plankton counter: the laser-OPC. *J. Plankton Res.*, **26**, 1135–1145.

Hirst, A. G. and Bunker, A. J. (2003) Growth of marine planktonic copepods: global rates and patterns in relation to chlorophyll a, temperature, and body weight. *Limnol. Oceanogr.*, **48**, 1988–2010.

Hopcroft, R. R., Roff, J. C., and Lombard, D. (1998) Production of tropical copepods in Kingston Harbour, Jamaica: the importance of small species. *Mar. Biol.*, **130**, 593–604.

Hopcroft, R. R., Clarke, C., Nelson, R. J., and Raskoff, K. A. *et al.* (2005) Zooplankton communities of the Arctic's Canada Basin: the contribution by smaller taxa. *Polar Biol.*, **28**, 198–206.

Izett, R. W., Manning, C. C., Hamme, R. C., and Tortell, P. D. (2018) Refined estimates of net community production in the subarctic Northeast Pacific derived from ΔO2/Ar measurements with N2O-based corrections for vertical mixing. *Global Biogeochem. Cycles*, **32**, 326–350.

Jennings, S., Warr, K. J., and Mackinson, S. (2002) Use of size-based production and stable isotope analyses to predict trophic transfer efficiencies and predator-prey body mass ratios in food webs. *Mar. Ecol. Prog. Ser.*, **240**, 11–20.

Kang, Y. J., Noh, Y., and Yeh, S. W. (2010) Processes that influence the mixed layer deepening during winter in the North Pacific. *J. Geophys. Res. Ocean.*, **115**, 1–14.

Kelley, D. and Richards, C. (2020) oce: Analysis of Oceanographic Data. R package version 1.2-0. https://CRAN.R-project.org/package=oce.

Kerr, S. R. and Dickie, L. M. (2001) *The Biomass Spectrum: A Predator–Prey Theory of Aquatic Production*, Columbia University Press, New York.

Kiørboe, T. (2013) Zooplankton body composition. *Limnol. Oceanogr.*, **58**, 1843–1850.

Kiørboe, T. and Hirst, A. G. (2014) Shifts in mass scaling of respiration, feeding, and growth rates across life-form transitions in marine pelagic organisms. *Am. Nat.*, **183**, E118–E130.

Kwong, L. E., Suchy, K. D., Sastri, A. R., Dower, J. F., and Pakhomov, E. A. (2020) A comparison of mesozooplankton production estimates from Saanich Inlet (British Columbia, Canada) using the chitobiase and biomass size spectra approaches. *Mar. Ecol. Prog. Ser.*, **655**, 59–75.

Liu, H. and Hopcroft, R. R. (2007) A comparison of seasonal growth and development of the copepods *Calanus marshallae* and *C. pacificus* in the northern Gulf of Alaska. *J. Plankton Res.*, **29**, 569–581.

Liu, H. and Hopcroft, R. R. (2006) Growth and development of *Neocalanus flemingeri/plumchrus* in the northern Gulf of Alaska: validation of the artificial-cohort method in cold waters. *J. Plankton Res.*, **28**, 87–101.

Lotze, H. K., Tittensor, D. P., Bryndum-Buchholz, A., Eddy, T. D., Cheung, W. W. L., Galbraith, E. D., Barange, M., Barrier, N., *et al.* (2019) Global ensemble projections reveal trophic amplification of ocean biomass declines with climate change. *Proc. Natl. Acad. Sci. U. S. A.*, **116**, 12907–12912.

Mack, H. R., Conroy, J. D., Blocksom, K. A., Stein, R. A., and Ludsin, S. A. (2012) A comparative analysis of zooplankton field collection and sample enumeration methods. *Limnol. Oceanogr. Methods*, **10**, 41–53.

Mackas, D. L., Thomson, R. E., and Galbraith, M. (2001) Changes in the zooplankton community of the British Columbia continental margin, 1985-1999, and their covariation with oceanographic conditions. *Can. J. Fish. Aquat. Sci.*, **58**, 685–702.

Mackas, D. L. (1992) Seasonal cycle of zooplankton off southwestern British Columbia: 1979-89. *Can. J. Fish. Aquat. Sci.*, **49**, 903–921.

Mackas, D. L. and Tsuda, A. (1999) Mesozooplankton in the eastern and western subarctic Pacific: community structure, seasonal life histories, and interannual variability. *Prog. Oceanogr*, **43**, 335–363.

Makabe, R., Tanimura, A., and Fukuchi, M. (2012) Comparison of mesh size effects on mesozooplankton collection efficiency in the Southern Ocean. *J. Plankton Res.*, **34**, 432–436.

Marcolin, C. R., Schultes, S., Jackson, G. A., and Lopes, R. M. (2013) Plankton and seston size spectra estimated by the LOPC and ZooScan in the Abrolhos Bank ecosystem (SE Atlantic). *Cont. Shelf Res.*, **70**, 74–87.

McAllister, C. D. (1961) Zooplankton studies at Ocean Weather Station 'P' in the Northeast Pacific Ocean. *J. Fish. Res. Board Canada*, **18**, 1–29.

Mehner, T., Lischke, B., Scharnweber, K., Attermeyer, K., Brothers, S., Gaedke, U., Hilt, S., and Brucet, C. (2018) Empirical correspondence between trophic transfer efficiency in freshwater food webs and the slope of their size spectra. *Ecology*, **99**, 1463–1472.

Moore, S. K. and Suthers, I. M. (2006) Evaluation and correction of subresolved particles by the optical plankton counter in three

Australian estuaries with pristine to highly modified catchments. *J. Geophys. Res. Ocean.*, **111**, 1–14.

Moriarty, R. and O'Brien, T. D. (2013) Distribution of mesozooplankton biomass in the global ocean. *Earth Syst. Sci. Data*, **5**, 45–55.

Nichols, J. H. and Thompson, A. B. (1991) Mesh selection of copepodite and nauplius stages of four calanoid copepod species. *J. Plankton Res.*, **13**, 661–671.

Nogueira, E., González-Nuevo, G., Bode, A., Varela, M., Morán, X. A. G., and Valdés, L. (2004) Comparison of biomass and size spectra derived from optical plankton counter data and net samples: application to the assessment of mesoplankton distribution along the Northwest and North Iberian Shelf. *ICES J. Mar. Sci.*, **61**, 508–517.

Oksanen, J., Blanchet, F. G., Friendly, M., Kindt, R., Legendre, P., McGlinn, D., Minchin, P. R., and O'Hara, R. B. (2019) vegan: Community Ecology Package. R package version 2.5-6. https://CRAN.R-project.org/package=vegan.

Peña, M. A. and Varela, D. E. (2007) Seasonal and interannual variability in phytoplankton and nutrient dynamics along Line P in the NE subarctic Pacific. *Prog. Oceanogr.*, **75**, 200–222.

Platt, T. and Denman, K. L. (1978) The structure of pelagic marine ecosystems. *Rapp. p.-v. réun. - Cons. int. Explor. mer*, **173**, 60–65.

Quiroga, E., Gerdes, D., Montiel, A., Knust, R., and Jacob, U. (2014) Normalized biomass size spectra in high Antarctic macrobenthic communities: linking trophic position and body size. *Mar. Ecol. Prog. Ser.*, **506**, 99–113.

R Core Team (2017) *R: A Language and Environment for Statistical Computing*, R Foundation for Statistical Computing.

Richon, C., Aumont, O., and Tagliabue, A. (2020) Prey stoichiometry drives iron recycling by zooplankton in the Global Ocean. *Front. Mar. Sci.*, **7**, 1–12.

Rossberg, A. G., Gaedke, U., and Kratina, P. (2019) Dome patterns in pelagic size spectra reveal strong trophic cascades. *Nat. Commun.*, **10**, 1–11.

Saito, R., Yamaguchi, A., Saitoh, S. I., Kuma, K., and Imai, I. (2011) East-west comparison of the zooplankton community in the subarctic Pacific during summers of 2003-2006. *J. Plankton Res.*, **33**, 145–160.

Saiz, E., Calbet, A., Irigoien, X., and Alcaraz, M. (1999) Copepod egg production in the western Mediterranean: response to food availability in oligotrophic environments. *Mar. Ecol. Prog. Ser.*, **187**, 179–189.

San Martin, E., Irigoien, X., Harris, R. P., López-Urrutia, Á., Zubkov, M. V., and Heywood, J. L. (2006) Variation in the transfer of energy in marine plankton along a productivity gradient in the Atlantic Ocean. *Limnol. Oceanogr.*, **51**, 2084–2091.

Sastri, A. R., Nelson, R. J., Varela, D. E., Young, K. V., Wrohan, I., and Williams, J. W. *et al.* (2012) Variation of chitobiase-based estimates of crustacean zooplankton production rates in high latitude waters. *J. Exp. Mar. Bio. Ecol.*, **414–415**, 54–61.

Sastri, A. R. and Dower, J. F. (2006) Field validation of an instantaneous estimate of in situ development and growth for marine copepod communities. *Can. J. Fish. Aquat. Sci.*, **63**, 2639–2647.

Sastri, A. R. and Dower, J. F. (2009) Interannual variability in chitobiase-based production rates of the crustacean zooplankton community in the Strait of Georgia. *Mar. Ecol. Prog. Ser.*, **388**, 147–157.

Sheldon, R. W., Prakash, A., and Sutcliffe, H. (1972) The size distribution of particles in the ocean. *Limnol, Oceanogr.*, **XVII**, 327–340.

Skjoldal, H. R., Wiebe, P. H., Postel, L., Knutsen, T., Kaartvedt, S., and Sameoto, D. (2013) Intercomparison of zooplankton (net) sampling systems: results from the ICES/GLOBEC Sea-going workshop. *Prog. Oceanogr.*, **108**, 1–42.

Sprules, W. G., Barth, L. E., and Giacomini, H. (2016) Surfing the biomass size spectrum: some remarks on history, theory, and application [1]. *Can. J. Fish. Aquat. Sci.*, **73**, 477–495.

Sprules, W. G. and Goyke, A. P. (1994) Size-based structure and production in the pelagia of lakes Ontario and Michigan. *Can. J. Fish. Aquat. Sci.*, **51**, 2603–2611.

Strickland, J. D. H. and Parsons, T. R. (1972) A practical handbook of seawater analysis. *Bull. Fish. Res. Board Canada*, 2nd edn, 167 pp.

Suchy, K. D., Dower, J. F., Varela, D. E., and Lagunas, M. G. (2016) Interannual variability in the relationship between in situ primary productivity and somatic crustacean productivity in a temperate fjord. *Mar. Ecol. Prog. Ser.*, **545**, 91–108.

Suthers, I. M., Taggart, C. T., Kelley, D., Rissik, D., and Middleton, J. H. (2004) Entrainment and advection in an island's tidal wake, as revealed by light attenuance, zooplankton and ichthyoplankton. *Limnol. Oceanogr.*, **49**, 283–296.

Thiebaux, M. L. and Dickie, L. M. (1992) Models of aquatic biomass size spectra and the common structure of their solutions. *J. Theor. Biol.*, **159**, 147–161.

Trudnowska, E., Basedow, S. L., and Błachowiak-Samołyk, K. (2014) Mid-summer mesozooplankton biomass, its size distribution, and estimated production within a glacial Arctic fjord (Hornsund, Svalbard). *J. Mar. Syst.*, **137**, 55–66.

Trudnowska, E., Stemmann, L., Błachowiak-Samołyk, K., and Kwasniewski, S. (2020) Taxonomic and size structures of zooplankton communities in the fjords along the Atlantic water passage to the Arctic. *J. Mar. Syst.*, **204**, 103306.

Turner, J. T. (2004) The importance of small planktonic copepods and their roles in pelagic marine food webs. *Zool. Stud.*, **43**, 255–266.

Vandromme, P., Nogueira, E., Huret, M., Lopez-Urrutia, A., González-Nuevo González, G., Sourisseau, M., and Petitgas, P. (2014) Springtime zooplankton size structure over the continental shelf of the Bay of Biscay. *Ocean Sci.*, **10**, 821–835.

Whitaker, D. and Christman, M. (2014) clustsig: Significant Cluster Analysis R package version 1.1. https://CRAN.R-project.org/package=clustsig.

Whitney, F. A., Crawford, D. W., and Yoshimura, T. (2005) The uptake and export of silicon and nitrogen in HNLC waters of the NE Pacific Ocean. *Deep. Res. Part II Top. Stud. Oceanogr.*, **52**, 1055–1067.

Wu, D., Zhou, M., Pierce, S. D., Barth, J. A., and Cowles, T. (2014) Zooplankton distribution and transport in the California Current off Oregon. *Mar. Ecol. Prog. Ser.*, **508**, 87–103.

Wu, J., Calvert, S. E., and Wong, C. S. (1997) Nitrogen isotope variations in the subarctic Northeast Pacific: relationships to nitrate utilization and trophic structure. *Deep. Res. Part I Oceanogr. Res. Pap.*, **44**, 287–314.

Zhou, M. (2006) What determines the slope of a plankton biomass spectrum? *J. Plankton Res.*, **28**, 437–448.